Magnetoplasmonics

Deutsche Ausgabe: DOI: 10.1002/ange.201508801
Internationale Ausgabe: DOI: 10.1002/anie.201508801

Electrochemiluminescent Spin-Polarized Modulation by Magnetic Ions and Surface Plasmon Coupling

Yun Shan, Hongyi Wu, Shijie Xiong, Xinglong Wu, and Paul K. Chu*

Integration of semiconductor nanocrystals (NCs) with metallic nanoparticles (NPs) enables light-emission modulation by surface plasmons[1] and provides the opportunity to modify the emission response from NCs through the interaction between an applied magnetic field and surface plasmons.[2] Thus, light emission influenced by a magnetic field can be exploited in optical sensing of magnetic biological processes. Although sensing of bio-substances with magnetism, such as hemoglobin and bio-reactions yielding magnetism changes, needs a weak magnetic field, it is fundamentally challenging to produce effective magnetic biosensing devices. In principle, magnetic field effects can occur by spin-dependent excitation and recombination.[2b,c,e] For example, spin-polarized hole injection from the cobalt nanocluster anode into an organic semiconductor poly[2-methoxy-5-(2′-ethylhexyloxy)-1,4-phenylenevinylene] layer can increase the electroluminescence efficiency by 18% at a field of 450 Oe by direct spin manipulation in the excitation process.[2f] The magnetic field effects can also be enhanced by integrating the light emission system with surface plasmons in metallic nanostructures.[1b,c] Recently, it has been demonstrated that a weak external magnetic field as small as 10 mT can modulate the wavevector of surface plasmons in a magnetoplasmonic structure (Au/Fe/Au and Au/Co/Au trilayer film),[3] and magnetic nanostructured iron oxide can also greatly enhance localized surface plasmon (LSP) resonance without an external field.[4]

Electrochemiluminescence (ECL), an electrically generated light emission process, involves light emission from the excited state of a luminophore owing to an initial electrochemical reaction on the electrode surface.[5] Semiconducting NCs possessing the ECL activity are promising ECL emitters in biosensing applications owing to simple surface functionalization and tunable ECL properties.[6] Particularly, light emission from semiconducting NCs can be easily modulated by surface plasmons in the metal nanostructures by a rational design.[1a,b] Metalloporphyrins such as iron (II) porphyrin and magnesium porphyrin with irreplaceable bio-functions play an important role in modern biological chemistry. Many metalloporphyrins have magnetism and undergo magnetism change when they specifically recognize diatomic molecular species.[7] In a solution, addition of one axial NO ligand, a ubiquitous signaling molecule in biology, can cause spin state change of manganese(II) tetraphenylporphyrin from $S = 2/5$ to $S = 0$.[7a,c] These results indicate that many bio-reactions can alter the magnetism of magnetic bio-substances significantly and sensitive detection of magnetic changes can be exploited to detect and recognize bio-molecules. In this work, we design an ECL-surface plasmon-coupled system consisting of semiconductor CdS NC film-Au NPs with DNA double strands (dsDNAs) as the linker (Figure 1). Using 5,10,15,20-tetra-(4-pyridyl)porphyrin (TPyP) as a model substance, ECL from the CdS NC film-Au NP system is controllably quenched by addition of Co ions under no applied magnetic field, and partially restored by adding Co-TPyP complexes. The magnetic ion-induced ECL modulation is attributed to the variation in the spin-dependent recombination rate owing to the internal magnetic field arising from the ferromagnetically aligned magnetic ions under the interaction with electron spins in Au NP. The methodology and results reported herein are expected to have potential biosensing applications.

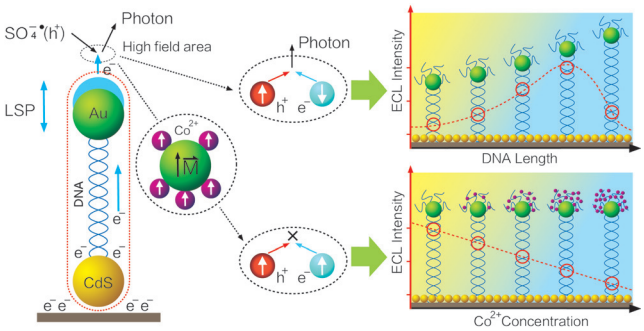

Figure 1. Diagram of the ECL process in the CdS NC film-Au NP coupling system in the presence of Co^{2+}. The surface plasmon is mainly localized close to the Au NPs and total magnetic moment of Co^{2+} in the ferromagnetic alignment act on the electrons and holes in the high-field area of the Au surface plasmon where radiative recombination takes place depending on spin-polarized modulation. The ECL intensity depends on the length of DNA double strands and decreases with increasing Co^{2+} concentration.

[*] Y. Shan, H. Y. Wu, Prof. S. J. Xiong, Prof. X. L. Wu
Key Laboratory of Modern Acoustics, MOE
Institute of Acoustics and Collaborative Innovation Center of Advanced Microstructures
Nanjing University
Nanjing 210093 (P.R. China)
E-mail: hkxlwu@nju.edu.cn
Y. Shan
Key Laboratory of Advanced Functional Materials of Nanjing
Nanjing Xiaozhuang University
Nanjing 211171 (P.R. China)
Prof. P. K. Chu
Department of Physics and Materials Science
City University of Hong Kong
Tat Chee Avenue, Kowloon, Hong Kong (China)

Supporting information for this article is available on the WWW under http://dx.doi.org/10.1002/anie.201508801.

The CdS NCs and 5 nm Au NPs (Supporting Information, Figure S1) are synthesized following reported methods,[8] and details regarding the NC film fabrication and assembly process are described in the Supporting Information (Experimental Section and Table S1). ECL modulation occurs when the Au NPs are connected to the CdS NC film. The Au NPs linked by dsDNAs of 27, 30, 36, 42, and 48 base pairs (bps) lead to 1.3, 2.7, 6, 9, and 3-fold ECL enhancements, respectively. The pristine CdS NC film can produce strong and stable ECL emission in the presence of co-reactant $S_2O_8^{2-}$ by the reaction involving electrochemical-reduction-generated $CdS^{-\cdot}$ and $SO_4^{-\cdot}$.[8a,9] The assembly of 3-mercaptopropionic acid (MPA), captured single-stranded DNA (CssDNA), dsDNA (42 bps), and bovine serum albumin (BSA) on the surface of the NC film hardly changes the ECL intensity (distinguished by the ECL peak height), while a 9-fold ECL enhancement is observed if the Au NPs are attached (Figure 2a). The results indicate that biomolecules on the CdS NC surface cannot effectively change the ECL intensity of the NC film. The ECL intensity of the CdS NC film is correlated with the reduction of co-reactant $S_2O_8^{2-}$. When MPA, CssDNA, BSA, dsDNAs, and Au NPs are attached to the surface of the CdS NC film in sequence, only very small variations are observed from the reduction peak potential and current of $S_2O_8^{2-}$ in the cyclic voltammograms (Supporting Information, Figure S2). This supports that ECL enhancement by Au NPs is not due to the small change in the reduction peak of $S_2O_8^{2-}$.

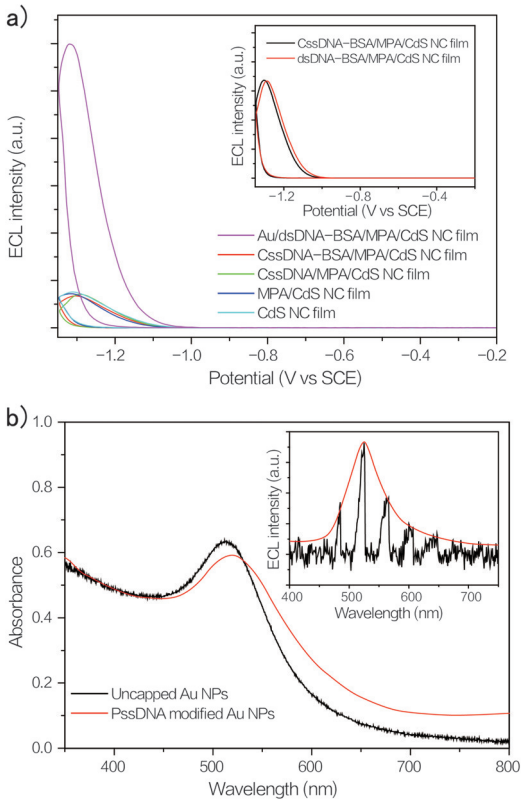

Figure 2. Cyclic ECL curves and UV/Vis absorption spectra acquired from the composite films. a) Cyclic ECL curves of the CdS NC film, MPA/CdS NC film, CssDNA/MPA/CdS NC film, Au/dsDNA-BSA/MPA/CdS NC film, CssDNA-BSA/MPA/CdS NC film (inset), and dsDNA-BSA/MPA/CdS NC film (inset). dsDNA: 42 bps, Scanning rate: 0.1 $V s^{-1}$. b) UV/Vis absorption spectra obtained from the uncapped and probing single-stranded DNA (PssDNA)-modified Au NPs. Inset: ECL spectrum of the CdS NC film.

As shown in the inset of Figure 2b, the ECL emission maximum from the NC film is at 524 nm and coincidentally in good agreement with the surface plasmon band of probing single-stranded DNA (PssDNA)-modified Au NPs at 522 nm which is slightly red-shifted compared to the pristine Au NPs (512 nm, Figure 2b), owing to enhancement of Au 5d band screening of 6s electron surface plasmon oscillations.[10] Therefore, the LSP in the Au NP can be coupled to electron-hole pairs or excitons in the NCs created by the electrical voltage and takes part in the ECL process to produce the ECL enhancement. The LSP is the collective oscillation of the electron cloud (with negative charge) in the Au NP along the DNA chain direction (Figure 1), while the core of NP (with positive charge) is stationary. In the semiperiod in which the electron cloud moves upward, there are empty electron orbitals in the lower half-sphere of the Au NP. The electrons in the CdS NCs on the cathode can swarm into these orbitals through the DNA chain and create momentum in the electron cloud to promote LSP oscillation. The magnitude of the momentum increases with the DNA length because for a longer distance, more work is done by the applied electric field. In the other semiperiod, the electron cloud conversely moves downward, but no electrons are injected into the CdS NCs because the states are already occupied by electrons owing to the attachment to the cathode. In this process, both the oscillation and electron cloud in the LSP increase, and the process ceases when the electron cloud is large enough to occupy all the available empty orbitals in the conduction band of the Au NP.[11] If the extra electrons on the NP can be neutralized by radiative recombination with holes carried by the complexes $SO_4^{-\cdot}$ in the solution, the aforementioned process continues and stabilizes. This can happen because there are many $SO_4^{-\cdot}$ complexes attracted by the negative NPs, and a high-field area may appear near the NPs owing to the effect of the LSP (Figure 1), which increases the probability of radiative recombination of holes on the $SO_4^{-\cdot}$ complexes and extra electrons on the NPs.

As demonstrated in Section S1 in the Supporting Information, radiation is annihilated when α or δ is small. Here, α is the promoting rate of the electron current through the DNA to the LSP oscillation and increases with length of the DNA chain. δ is the transmission rate of electrons through the DNA and becomes smaller with increasing length of DNA chain. This means that a moderate (neither short nor long) DNA chain may be suitable. Here, the maximum ECL enhancement factor is obtained with dsDNAs of 42 bps (Figure 2a). Different enhancement factors owing to the difference in the surface plasmon bands are ruled out as the Au NPs modified with PssDNA of different bases show nearly the same surface plasmon bands. Hence, the DNA lengths result in different enhancement factors.

Radiative recombination of electrons and holes happens in narrow high-field areas near the Au NPs (Figure 1). This provides the possibility to control the recombination and

luminescence strength by means of an internal magnetic field concentrated near the Au NPs. Here, ECL modulation of the CdS NC film-Au NP coupled system with dsDNA of 42 bps as the linker by Co^{2+} with intrinsic magnetic moments is investigated. The effect of 100 μM Co^{2+} on this coupled system is shown in Figure 3a. The ECL intensity decreases by

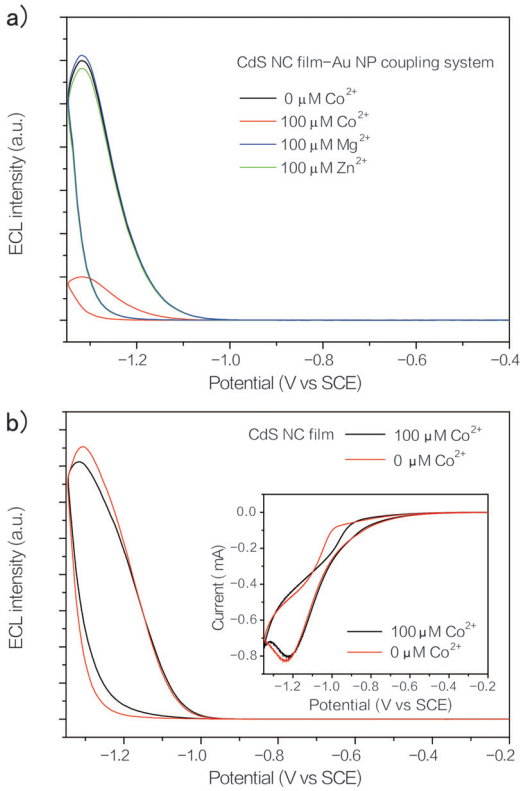

Figure 3. Cyclic ECL curves obtained after addition of Co^{2+}, Zn^{2+} and Mg^{2+}. a) Effects of 100 μM Co^{2+}, Zn^{2+}, and Mg^{2+} on the ECL intensity of the Au/dsDNA(42 bps)-BSA/MPA/CdS NC film (CdS NC film-Au NP coupling system). b) Effects of Co^{2+} on the pristine CdS NC film. Inset: Typical cyclic voltammograms of $S_2O_8^{2-}$ before and after addition of 100 μM Co^{2+} to the ECL system. Scanning rate: 0.1 Vs^{-1}.

83% in the presence of 100 μM Co^{2+}. In the control experiments, only about 7% quenching of the ECL intensity is observed from the pristine CdS NC film in the presence of 100 μM Co^{2+} (Figure 3b). 100 μM of Co^{2+} result in less than 10% decrease in the ECL intensity of the CdS NC film modified by dsDNAs without Au NPs (not shown). The inset in Figure 3b shows the typical cyclic voltammograms of $S_2O_8^{2-}$ before and after addition of 100 μM Co^{2+} to the ECL system. Obviously, Co^{2+} only causes a very small change in the reduction peak current and potential of $S_2O_8^{2-}$, indicating that ECL quenching of the coupled system cannot be attributed to Co^{2+}-induced change in the reduction of $S_2O_8^{2-}$. Control experiments involving nonmagnetic Zn^{2+} and Mg^{2+} show that 100 μM Zn^{2+} or Mg^{2+} produces very small changes in the ECL intensity (Figure 3a). Thus, the large ECL quenching is mainly due to spin polarization of electrons and holes caused by the internal magnetic field from Co^{2+} in the vicinity of Au NPs. It reduces the amount of e-h pairs with the inverse spin orientation.[2b,c,e] ECL quenching of the CdS NC film-Au NP system also works with magnetic Fe^{2+} and Fe^{3+} as 100 μM Fe^{2+} and Fe^{3+} decrease the ECL intensity by 80% and 75%, respectively (Supporting Information, Figure S3).

To further clarify the magnetic effect of Co^{2+}, UV/Vis absorption of PssDNA-modified Au NPs was monitored before and after addition of 100 μM Co^{2+}. There was no noticeable shift, and only a very small intensity change in the surface plasmon band (Supporting Information, Figure S3), indicating that no change occurs in the spectral overlapping of ECL and surface plasmon of Au NPs. The very small change in the surface plasmon resonance peak intensity implies that the influence of magnetic Co^{2+} on the UV/Vis absorption is negligible. The situation for 100 μM Zn^{2+} or Mg^{2+} is similar. No noticeable spectral shift or intensity change in the surface plasmon band were observed, indicative of the essential role of magnetic Co^{2+} in ECL quenching.

Co^{2+} is paramagnetic possessing an intrinsic magnetic moment. When some Co ions are in close proximity with an Au NP, the magnetic moments of Co^{2+} interact with spins of electrons in the Au NP and can be ferromagnetically aligned to produce a total magnetic moment **M**, as shown in Figure 1. If the magnetic interaction strengths on nearby electrons and holes are J_e and J_h, the recombination rate after spin modulation can be calculated by (Supporting Information, Section S2):

$$\gamma = \frac{2\gamma_0\left(e^{-2J_h\mu M/k_BT} + e^{-2J_e\mu M/k_BT}\right)}{(1+e^{-2J_e\mu M/k_BT})(1+e^{-2J_h\mu M/k_BT})},$$

where γ_o is the recombination rate in the absence of an internal magnetic field, μ is the magnetic moment of electron and hole, and k_B and T are the Boltzmann constant and temperature, respectively. The recombination rate and corresponding luminescence intensity will be quenched by the internal magnetic field by changing the spin polarization of electrons or holes because J_e and J_h are non-zero in the presence of magnetic Co^{2+}. Being in agreement with theoretical calculation, the ECL intensity of the CdS NC film-Au NP coupling system can be modulated by the concentration of Co^{2+}. When the concentration of Co^{2+} is reduced from 100 to 10 μM, the ECL quenching efficiency drops from 83% to 22% (Figure 4a). Co^{2+}-modulated ECL quenching is similar to the effect of an applied external magnetic field. External magnetic fields of 20 and 50 Gauss applied by the permanent magnet produce 67% and 94% decreases in the ECL intensity, respectively (Supporting Information, Figure S5), suggesting that Co^{2+} in close proximity with Au NPs may be ferromagnetically aligned by coupling with electron spins producing an internal magnetic field.

To explore the biosensing potential of the Co^{2+}-modulated ECL quenching effect, the ECL response of the CdS NC film-Au NP system to the Co^{2+}-TPyP interaction is monitored. Here, TPyP acts as a spacer. The complexes with Co^{2+} lessen the amount of Co^{2+} in close proximity with Au NPs, and thus decrease the total magnetic moment. This case is similar to that under the influence of an applied external magnetic field. In these experiments, we directly added Co^{2+} and TPyP to the ECL reaction system (pH 8.3). Figure 5a presents the

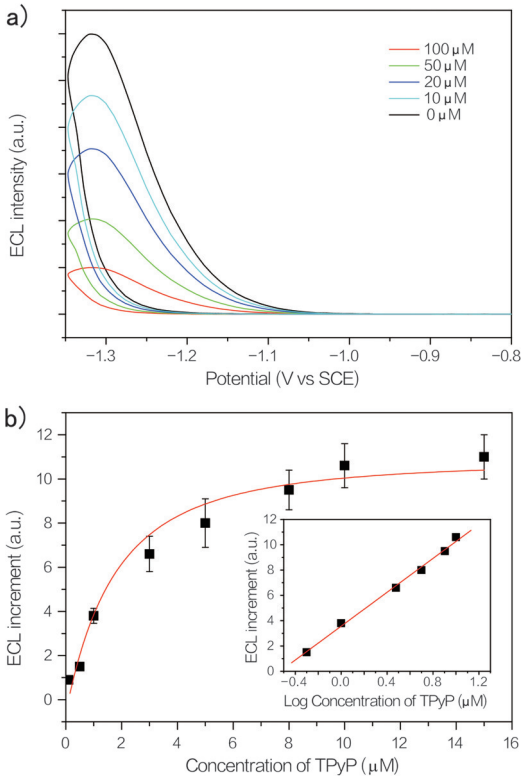

Figure 4. Cyclic ECL curves obtained in the presence of different Co^{2+} concentrations and dependence of the ECL increment on TPyP concentration. a) ECL modulation of the CdS NC film-Au NP coupling system for different Co^{2+} concentrations. dsDNA: 42 bps, Scanning rate: 0.1 Vs^{-1}. b) Relationship between the ECL increment observed from the CdS NC film-Au NP system in the presence of 100 μM Co^{2+} and different TPyP concentrations. Each data point represents the average of three measurements. The red line is the theoretical ECL intensity increment as a function of TPyP concentration. The parameters are: $T = 300$ K, $\kappa = 0.3$ μM, and $J_e\mu M_\nu = J_h\mu M_\nu = 0.01$ eV. Inset: Logarithmic calibration curve of TPyP. dsDNA: 42 bps.

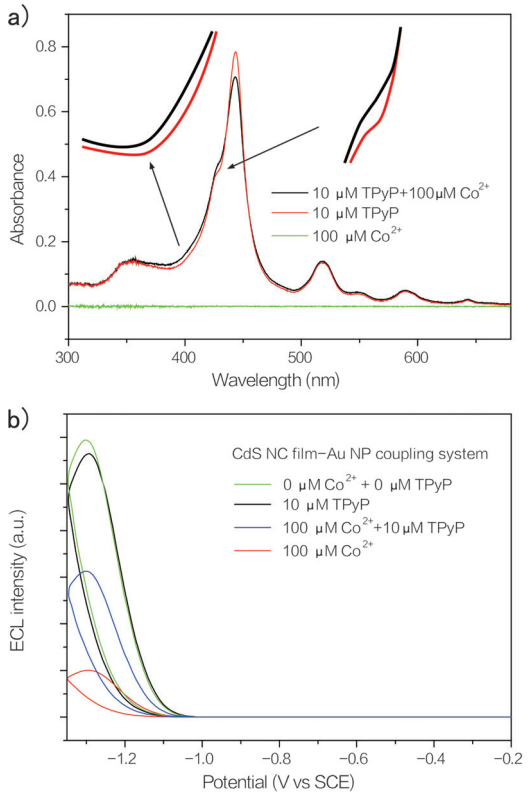

Figure 5. UV/Vis absorption spectra and cyclic ECL curves. a) Absorption spectra of 10 μM TPyP before and after addition of 100 μM Co^{2+}. b) Effects of TPyP on ECL of the CdS NC film-Au NP coupling system with and without 100 μM Co^{2+}.

electronic transition spectra of 100 μM Co^{2+}, 10 μM TPyP, and their mixture in the ECL detection buffer, respectively. Co^{2+} has no absorption in the UV to Vis spectral range. TPyP shows intense absorption at 440 nm with a shoulder at 425 nm for the Soret band and four less intense Q-bands between 500 and 650 nm. After further addition of Co^{2+}, the 440 nm absorption band decreases together with a larger and slightly red-shifted shoulder (right inset), indicating coordination between TPyP and Co^{2+}.[12] The increase in absorption at about 400 nm also confirms the occurrence of coordination (left inset)[13] and thus, the complexing reaction takes place between Co^{2+} and TPyP.

The effect of 10 μM TPyP on the ECL intensity of the CdS NC film-Au NP system (dsDNA of 42 bps) in the presence of 100 μM Co^{2+} is shown in Figure 5b. 10 μM TPyP leads to a small drop in the ECL intensity because TPyP has weak absorption in the ECL spectral range of the CdS NC film (Figure 5a). The effect of TPyP on the ECL reaction owing to electron transfer is ruled out in view of the nearly unchanged reduction peak potential and current of $S_2O_8^{2-}$ (not shown). Although either Co^{2+} or TPyP is an ECL quencher of the coupled system, 10 μM TPyP can recover the 100 μM Co^{2+}-quenched ECL from 17% to 52% of the initial value. Interestingly, smaller ECL quenching efficiency (50%) is observed when 10 μM TPyP is first added, followed by addition of 100 μM Co^{2+}. The results show that only those Co^{2+} ions non-complexed with TPyP and in close proximity to Au NPs can couple with the Au NPs to consequently produce ECL quenching.[14] Thus, the efficiency of ECL intensity recovery depends on the concentration of TPyP.

The relationship between the increase in the ECL intensity of the CdS NC film-Au NP coupled system in the presence of 100 μM Co^{2+} and TPyP concentrations (0.1–15 μM) is investigated. With increasing TPyP concentration, the ECL increment becomes larger and reaches a plateau at a TPyP concentration of 10 μM. The logarithmic calibration curve of ECL increment versus TPyP concentration exhibits good linearity in the range of 0.5–10 μM (coefficient of determination $R^2 = 0.996$; inset of Figure 4b). The favorable response of 0.1 μM TPyP indicates a remarkable response of this system to magnetic changes (signal/noise S/N = 3). Additionally, the ECL intensity of the CdS NC film-Au NP-coupled system can be fully restored by washing away Co^{2+} and Co-TPyP complexes. As shown in Section S3 in the Supporting Information, we theoretically calculate the dependence of the ECL intensity on the Co^{2+} (TPyP) concentration in the solution. The calculation results are also presented in Figure 4b for comparison (red line). By

increasing the Co^{2+} (TPyP) concentration, the ECL intensity increases. The increase is finally saturated at a large TPyP concentration, in very good accordance with our experimental results. It is also found that the 100 μM Co^{2+}-quenched ECL from the CdS NC film-Au NP system can be partially recovered by L-proline, a natural amino acid. The ECL quenching efficiency decreases from 83% to 35% by adding 10 μM L-proline (Supporting Information, Figure S6). It provides evidence about the large potential of the system pertaining to the detection of biomolecules.

In conclusion, luminescent semiconducting NC film/metallic NPs with strong surface plasmons constitute an experimentally simple and efficient ECL system to achieve magnetic biosensing by combining with magnetic ions only. This system not only offers a good theoretical model to understand the influence of the local magnetic field on radiative recombination of electrons and holes in close proximity to metallic NPs, but also renders magnetic biosensing possible. It may be possible to increase the detection sensitivity by changing the size and morphology of the metallic NPs or using ultra-thin magnetic nanoclusters in a solution.

Acknowledgements

This work was supported by National Basic Research Programs of China under Grant Nos. 2014CB339800 and 2013CB932901 and National Natural Science Foundation of China (Nos. 11374141, 21203098, 61521001, and 21375067). Partial support was also from Qing Lan Project of Jiangsu Province and China Postdoctoral Science Foundation (2013M530247), as well as City University of Hong Kong Strategic Research Grant (SRG) No. 7004188.

Keywords: biosensing · electrochemiluminescence · spin-polarized modulation · surface plasmon coupling

How to cite: *Angew. Chem. Int. Ed.* **2016**, *55*, 2017–2021
Angew. Chem. **2016**, *128*, 2057–2061

[1] a) L. L. Li, Y. Chen, Q. Lu, J. Ji, Y. Y. Shen, M. Xu, R. Fei, G. H. Yang, K. Zhang, J. R. Zhang, J. J. Zhu, *Sci. Rep.* **2013**, *3*, 1529; b) X. Zhang, C. A. Marocico, M. Lunz, V. A. Gerard, Y. K. Gun'ko, V. Lesnyak, N. Gaponik, A. S. Susha, A. L. Rogach, A. L. Bradley, *ACS Nano* **2012**, *6*, 9283–9290; c) J. Yoo, X. D. Ma, W. Tang, G.-C. Yi, *Nano Lett.* **2013**, *13*, 2134–2140; d) G. J. Tian, J. C. Liu, Y. Luo, *Phys. Rev. Lett.* **2011**, *106*, 177401; e) V. Temnov, U. Woggon in *Quantum dots*: *optics*, *electron transport and future applications*, Chap. 11 (Ed.: A. Tartakovski), Cambridge University Press, Cambridge, **2012**, pp. 185–197; f) O. Kulakovich, N. Strekal, A. Yaroshevich, S. Maskevich, S. Gaponenko, I. Nabiev, U. Woggon, M. Artemyev, *Nano Lett.* **2002**, *2*, 1449–1452.

[2] a) T. D. Nguyen, G. Hukic-Markosian, F. J. Wang, L. Wojcik, X.-G. Li, E. Ehrenfreund, Z. V. Vardeny, *Nat. Mater.* **2010**, *9*, 345–352; b) M. Shao, L. Yan, H. P. Pan, I. Ivanov, B. Hu, *Adv. Mater.* **2011**, *23*, 2216–2220; c) C. Zhang, D. Sun, C.-X. Sheng, Y. X. Zhai, K. Mielczarek, A. Zakhidov, Z. V. Vardeny, *Nat. Phys.* **2015**, *11*, 427–434; d) M. Kataja, T. K. Hakala, A. Julku, M. J. Huttunen, S. van Dijken, P. Törmä, *Nat. Commun.* **2015**, *6*, 7072; e) S. van Reenen, S. P. Kersten, S. H. W. Wouters, M. Cox, P. Janssen, B. Koopmans, P. A. Bobbert, M. Kemerink, *Phys. Rev. B* **2013**, *88*, 125203; f) Y. Wu, B. Hu, J. Howe, A.-P. Li, J. Shen, *Phys. Rev. B* **2007**, *75*, 075413.

[3] a) E. Ferreiro-Vila, M. Iglesias, E. Paz, F. J. Palomares, F. Cebollada, J. M. González, G. Armelles, J. M. García-Martín, A. Cebollada, *Phys. Rev. B* **2011**, *83*, 205120; b) V. V. Temnov, G. Armelles, U. Woggon, D. Guzatov, A. Cebollada, A. Garcia-Martin, J.-M. Garcia-Martin, T. Thomay, A. Leitenstorfer, R. Bratschitsch, *Nat. Photonics* **2010**, *4*, 107–111.

[4] a) L. Tang, J. Casas, M. Venkataramasubramani, *Anal. Chem.* **2013**, *85*, 1431–1439; b) Z. Li, J. J. Foley IV, S. Peng, C.-J. Sun, Y. Ren, G. P. Wiederrecht, S. K. Gray, Y. G. Sun, *Angew. Chem. Int. Ed.* **2015**, *54*, 8948–8951; *Angew. Chem.* **2015**, *127*, 9076–9079.

[5] F. Pinaud, L. Russo, S. Pinet, I. Gosse, V. Ravaine, N. Sojic, *J. Am. Chem. Soc.* **2013**, *135*, 5517–5520.

[6] a) L. Y. Zheng, Y. W. Chi, Y. Q. Dong, J. P. Lin, B. B. Wang, *J. Am. Chem. Soc.* **2009**, *131*, 4564–4565; b) J. Tan, L. R. Xu, T. Li, B. Su, J. M. Wu, *Angew. Chem. Int. Ed.* **2014**, *53*, 9822–9826; *Angew. Chem.* **2014**, *126*, 9980–9984; c) H. Jiang, X. M. Wang, *Anal. Chem.* **2014**, *86*, 6872–6878; d) Y. Shan, J. J. Xu, H. Y. Chen, *Chem. Commun.* **2010**, *46*, 4187–4189; e) D. Jiang, X. J. Du, Q. Liu, L. Zhou, J. Qian, K. Wang, *ACS Appl. Mater. Interfaces* **2015**, *7*, 3093–3100; f) L. L. Li, K. P. Liu, G. H. Yang, C. M. Wang, J. R. Zhang, J. J. Zhu, *Adv. Funct. Mater.* **2011**, *21*, 869–878.

[7] a) S. R. Burema, K. Seufert, W. Auwärter, J. V. Barth, M. Bocquet, *ACS Nano* **2013**, *7*, 5273–5281; b) B. W. Heinrich, G. Ahmadi, V. L. Müller, L. Braun, J. I. Pascual, K. J. Franke, *Nano Lett.* **2013**, *13*, 4840–4843; c) N. Ballav, C. Wäckerlin, D. Siewert, P. M. Oppeneer, T. A. Jung, *J. Phys. Chem. Lett.* **2013**, *4*, 2303–2311.

[8] a) J. Wang, Y. Shan, W. W. Zhao, J. J. Xu, H. Y. Chen, *Anal. Chem.* **2011**, *83*, 4004–4011; b) A. Gole, C. J. Murphy, *Chem. Mater.* **2004**, *16*, 3633–3640.

[9] G. F. Jie, B. Liu, H. C. Pan, J. J. Zhu, H. Y. Chen, *Anal. Chem.* **2007**, *79*, 5574–5581.

[10] S. J. Park, R. E. Palmer, *Phys. Rev. Lett.* **2009**, *102*, 216805.

[11] a) V. Krachmalnicoff, E. Castanié, Y. De Wilde, R. Carminati, *Phys. Rev. Lett.* **2010**, *105*, 183901; b) F. Wang, Y. R. Shen, *Phys. Rev. Lett.* **2006**, *97*, 206806.

[12] V. Villari, P. Mineo, E. Scamporrino, N. Micali, *Chem. Phys.* **2012**, *402*, 118–123.

[13] T. Imaoka, H. Horiguchi, K. Yamamoto, *J. Am. Chem. Soc.* **2003**, *125*, 340–341.

[14] a) A. D. Zhao, Q. X. Li, L. Chen, H. J. Xiang, W. H. Wang, S. Pan, B. Wang, X. D. Xiao, J. L. Yang, J. G. Hou, Q. S. Zhu, *Science* **2005**, *309*, 1542–1544; b) Z. L. Shi, N. Lin, *J. Am. Chem. Soc.* **2009**, *131*, 5376–5377.

Received: September 19, 2015
Revised: November 22, 2015
Published online: December 28, 2015

